Coprecipitation of actinides peroxide salts in the U-Th and U-Pu systems and their thermal decomposition.

Nicolas Hibert [a,b], Bénédicte Arab-Chapelet [a], Murielle Rivenet [b], Laurent Venault [a], Christelle Tamain [a] and Olivier Tougait [b]*

Affiliation :

a) CEA, DES,ISEC,DMRC, Univ Montpellier, Marcoule, France

b) Univ. Lille, CNRS, Centrale Lille, Univ. Artois, UMR 8181 – UCCS – Unité de Catalyse et Chimie du Solide, F-59000 Lille, France

Supplementary Information

3.1 Precipitation of actinide peroxide salts: yields and filtering rates.

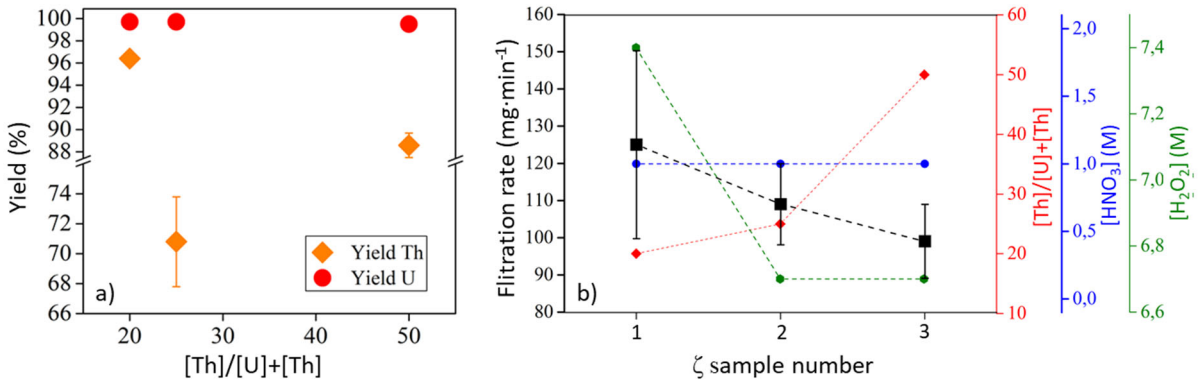

Figure S1 : a) Variation of the individual U peroxide and Th peroxide precipitation yields as function of the $\frac{[Th]}{[Th]+[U]}$ ratio. b) filtering rate (back square) of the mixed U peroxide and Th peroxide slurry according to the experimental conditions. The red, green and blue symbols stand for the $\frac{[Th]}{[Th]+[U]}$ ratio and the initial concentrations of [HNO_3] and [H_2O_2] respectively.

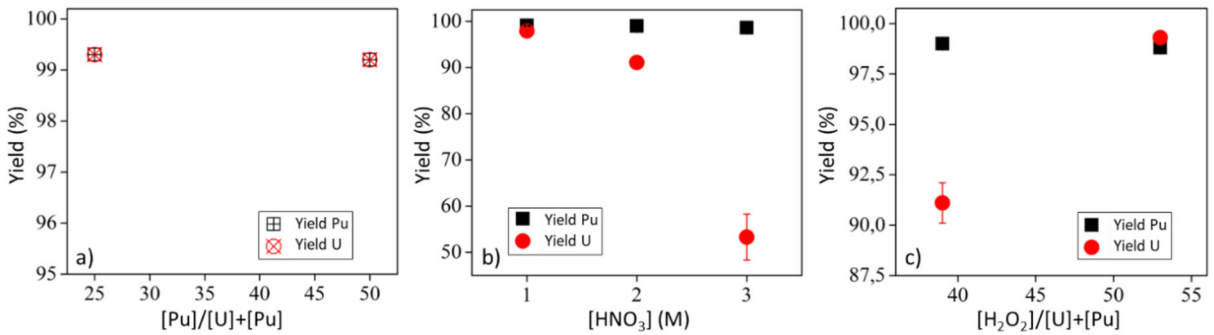

Figure S2 : Variation of the individual U peroxide and Pu peroxide precipitation yields as function of a) the [Pu]/[U]+[Pu] ratio, b) the initial nitric acid concentration and c) the [H_2O_2]/[U]+[Pu] ratio.

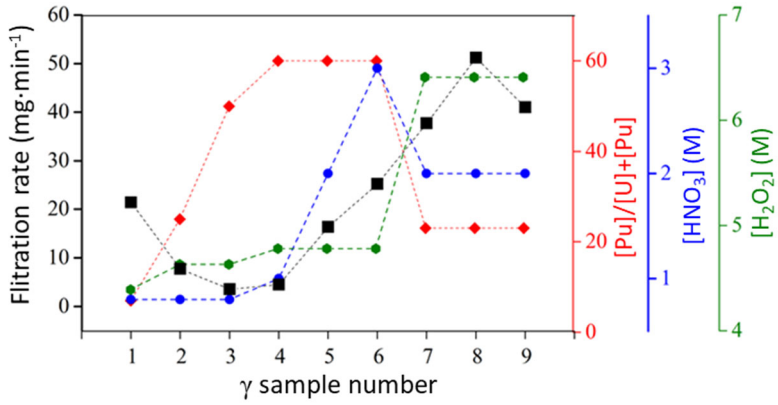

Figure S3: Filtering rate (back square) of the U peroxide and Pu peroxide slurry from the γ coprecipitation tests. The red, green and blue symbols stand for the [Pu]/[Pu]+[U] ratio and the initial concentrations of [HNO_3] and [H_2O_2] respectively.

3.2.1 Powder DRX

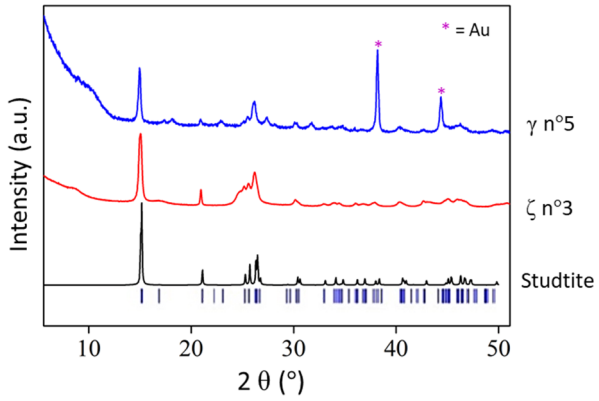

Figure S4: Powder X-ray diffraction pattern of γ n°5 and ζ n°3 compared to the calculated diffractogram of studtite [29].

3.2.2 Infrared and Raman spectroscopies

The IR spectra of the γ n°4 and γ n°5 precipitates are displayed in Figure S5 showing the uranyl ion antisymmetric stretching band at ν_{as} = 903 cm^{-1} with the symmetric stretching of peroxide ion at ν = 861 cm^{-1} [58], the nitrate ion stretching bands ν = 1404 cm^{-1}, 1333 cm^{-1} and 1040 cm^{-1} [60], the specific band attributed to plutonium peroxide at ν(A) = 832 cm^{-1} [45] and the absorption band at ρ_r (H_2O) = 726 cm^{-1} which can be ascribed to the presence of coordinated water [57,61] incorporated in studtite.

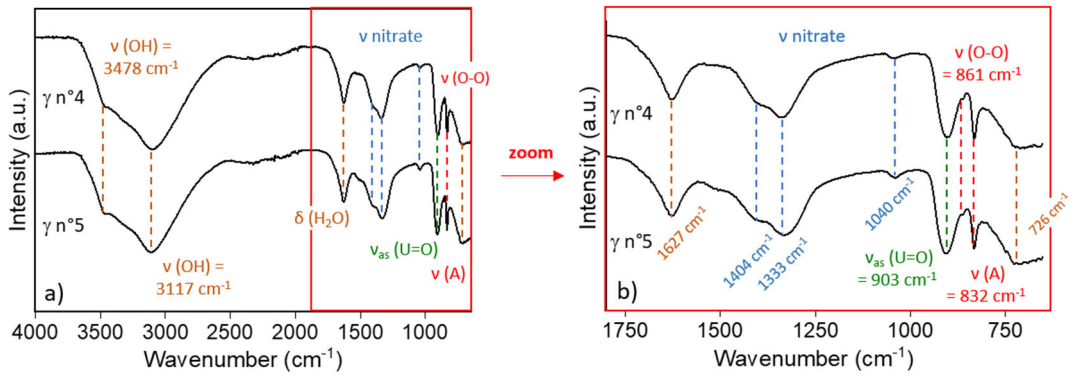

Figure S5 : Infrared spectra of γ n°4 and γ n°5 of U-Pu precipitation tests, along with signal assignment for the specific functional groups. a) whole spectra, b) enlarged area: 1800-650 cm-1

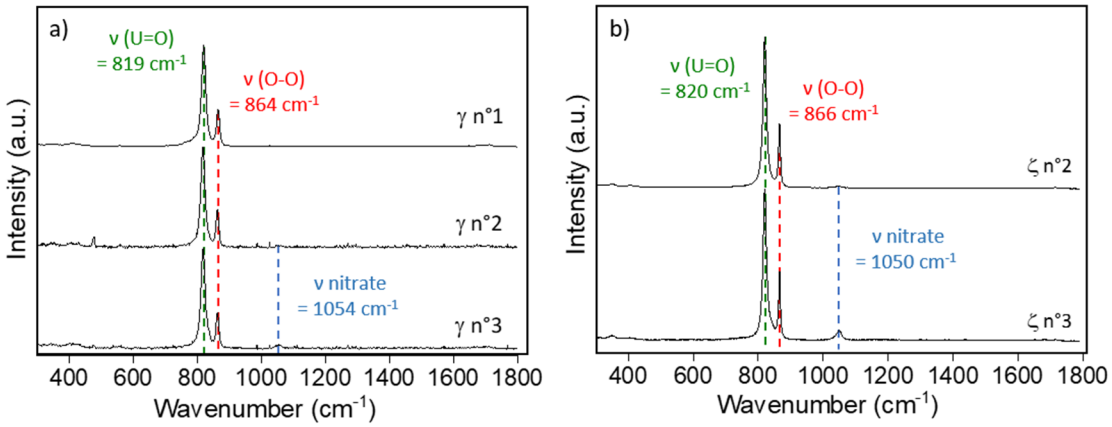

Figure S6 : Raman spectra along with signal assignment for the functional groups a) γ n°1, γ n°2 and γ n°3 of U-Pu precipitation tests, b) ζ n°2 and ζ n°3 of U-Th precipitation tests.

3.4.1 The U-Pu system

Rietveld analyses of the X-ray diffraction patterns of the thermal analysis solid residues of γ n°2 and γ n°3 were performed using FullProf [ref, 46]. Phase identification and refinement of the lattice parameters of each individual oxide phase were carried out, whereas the lattice parameter of gold was kept constant. The excluded regions correspond to diffraction peaks of the sample holder which has an unknown crystal structure.

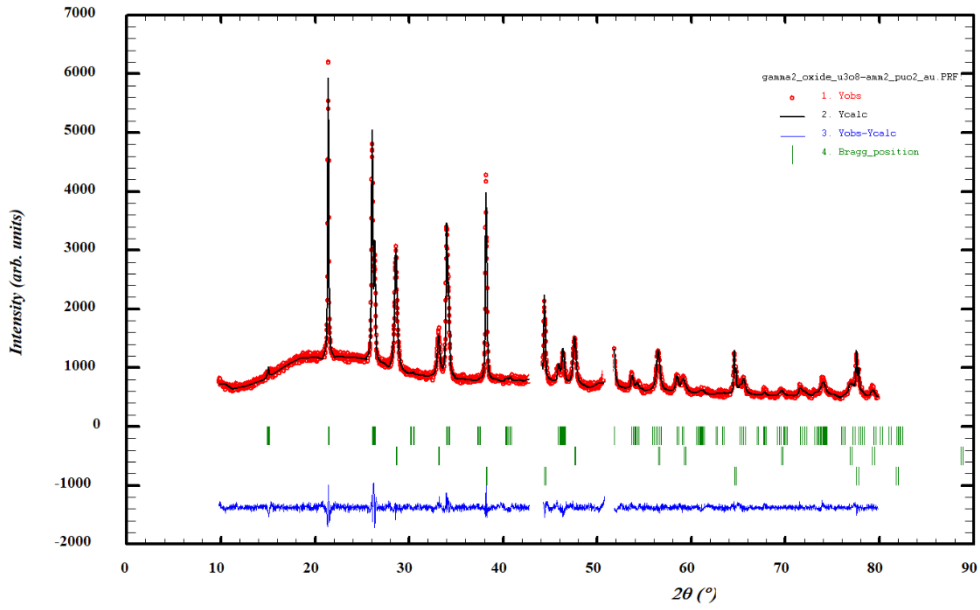

Figure S7 : Final Rietveld plot showing the observed, calculated and difference pattern for the γ n°2 residual powder. The Bragg reflections for crystalline phases are indicated by vertical bars, from top to bottom, α U_3O_8, PuO_2 and Au.

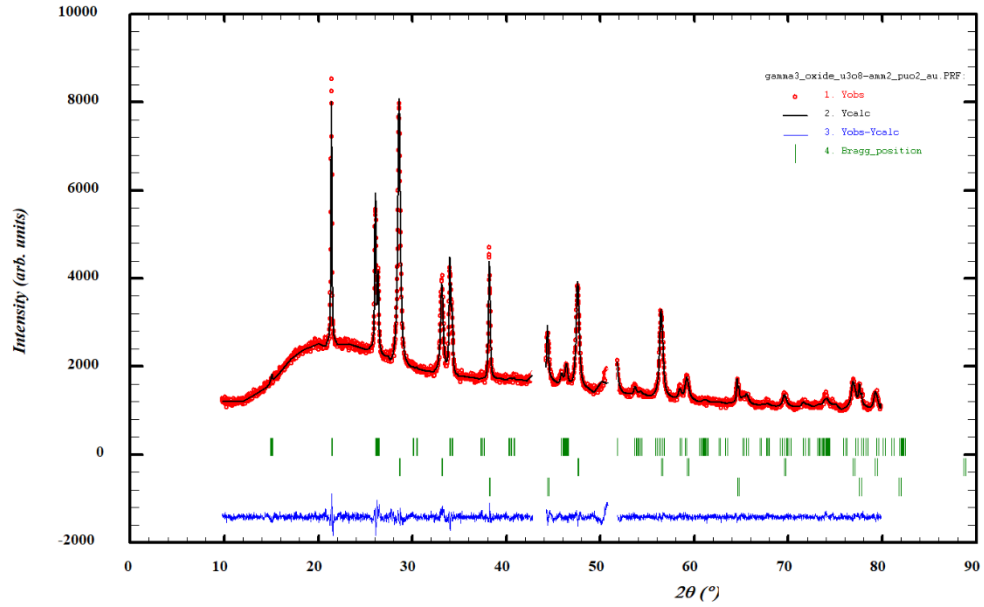

Figure S8 : Final Rietveld plot showing the observed, calculated and difference pattern for the γ n°3 residual powder. The Bragg reflections for crystalline phases are indicated by vertical bars, from top to bottom, α U_3O_8, PuO_2 and Au.

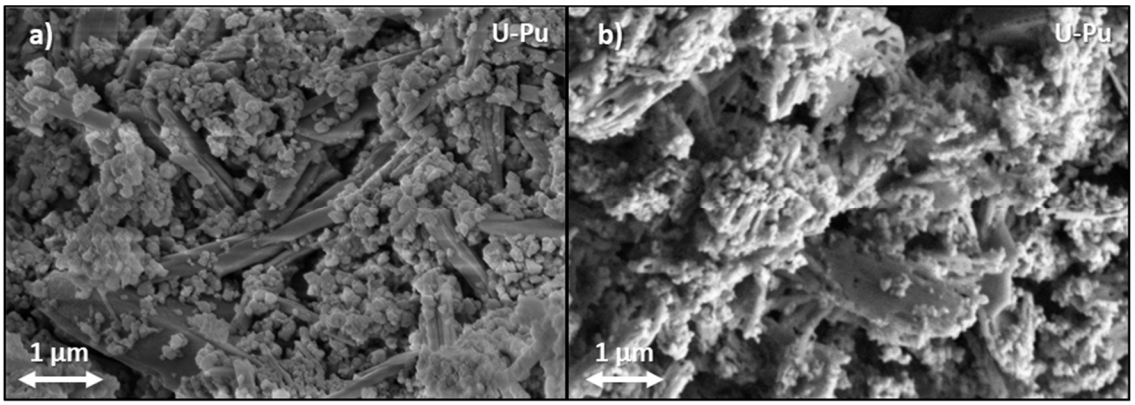

Figure S9 : SEM images in SE mode of γ n°5 test powder for a) as-precipitated (left) and b) calcined under air at 800°C (right)

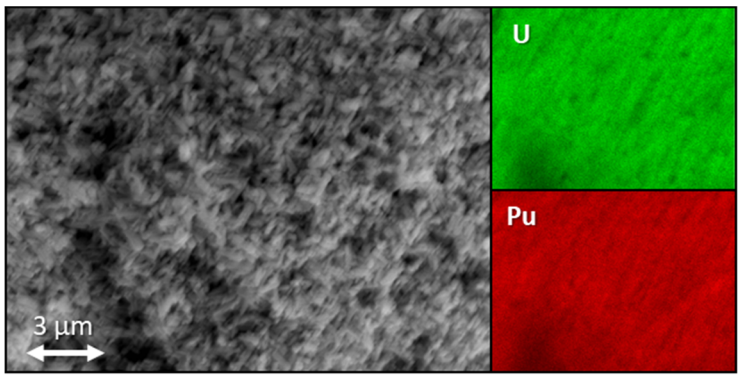

Figure S10 : X-EDS maps for U and Pu of the calcined γ n°5 powder at 800°C under air

3.4.2. The U-Th system

A Rietveld analysis of the X-ray diffraction patterns of the thermal analysis of solid residue of *ζ n°3* was performed using FullProf [ref, 46]. Phase identification and refinement of the lattice parameters of each individual oxide phase were carried out, whereas the lattice parameter of gold was kept constant. The excluded regions correspond to diffraction peaks of the sample holder which has an unknown crystal structure.

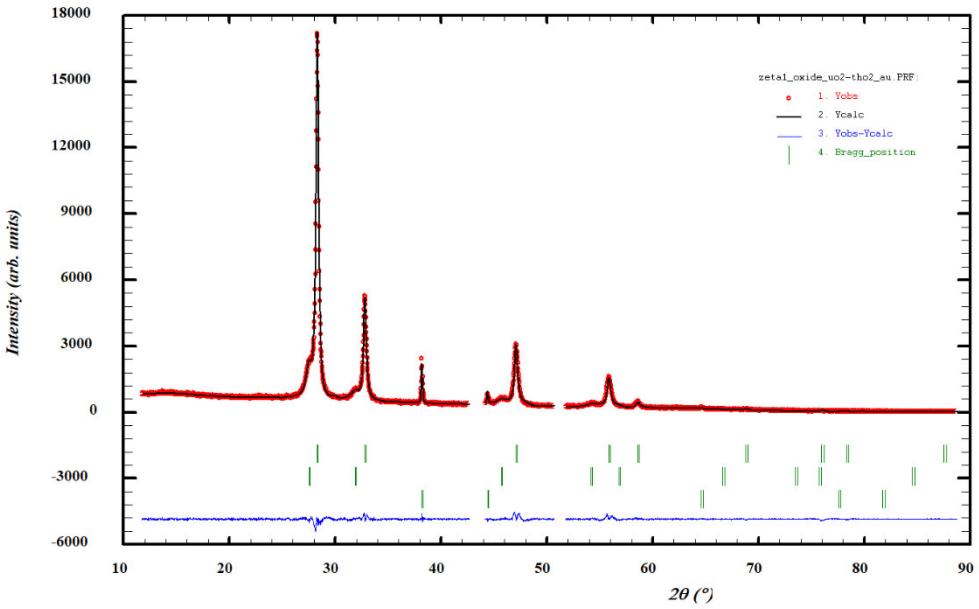

Figure S11: Final Rietveld plot showing the observed, calculated and difference pattern for the ζ n°3 residual powder. The Bragg reflections for crystalline phases are indicated by vertical bars, from top to bottom, UO_2, ThO_2 and Au.

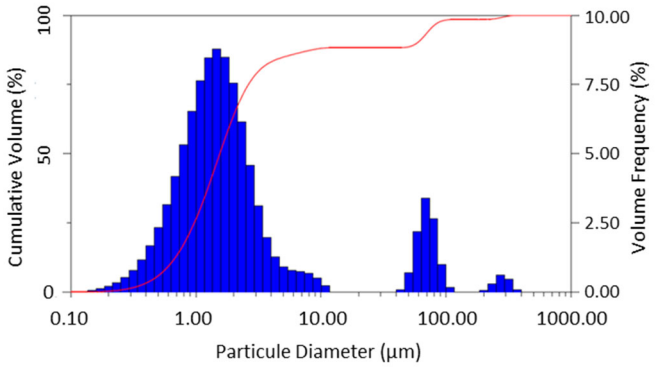

Figure S12: Particle Size Distribution (PSD) of U-Th oxides powder of the calcined ζ n°1 sample at 600°C under Ar+H_2 (5%)

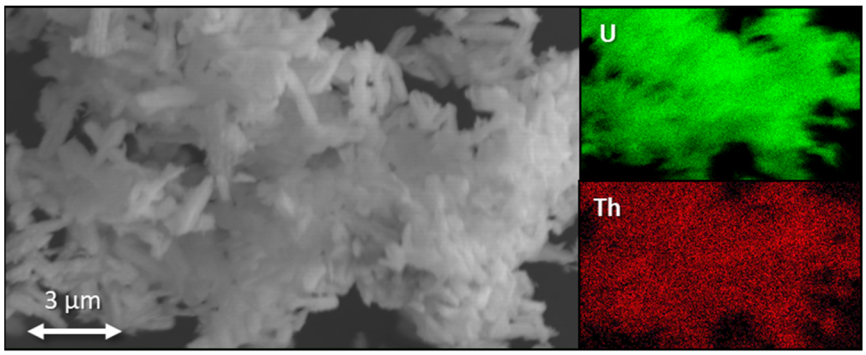

Figure S13 : X-EDS maps for U(Ma) and Th(La) of the oxide powder after calcination up to 1000°C under Ar+H_2 (5%) of ζ n°1 sample.